Contribution from the Inorganic Chemistry Laboratory,
University of Oxford, Oxford OX1 3QR, U.K.

Photochemical Studies of Rhenium η-Cyclopentadienyl Complexes in Matrices and in Solution: Detection of Rhenocene and Mechanisms of Hydrogen Transfer†

JENNIFER CHETWYND-TALBOT, PETER GREBENIK, ROBIN N. PERUTZ,* and MARK H. A. POWELL

Received August 23, 1982

The photochemistries of $ReCp_2H$ (**1**), $ReCp(CO)_3$ (**2**), and $ReCp(\eta^2\text{-}C_5H_6)(CO)_2$ (**3**) (Cp = η-C_5H_5) have been examined in low-temperature matrices. Complex **1** reacts by two competing pathways: (a) loss of hydrogen atoms (CO and N_2 matrices) leads to $ReCp_2$ (**4**) characterized by visible absorption, laser-excited fluorescence, and IR spectroscopy, assisted by ^2H substitution; (b) partial ring decoordination and concomitant ligand addition led to $ReCp(\eta^3\text{-}C_5H_5)(L)H$ (L = CO (**5**), N_2 (**6**)) characterized by IR spectroscopy using ^2H, ^{13}CO, and ^{15}N substitution. The photolysis of **2** (in Ar matrices) yields $ReCp(CO)_2$ (**7**) reversibly and (in N_2 matrices) $ReCp(CO)_2N_2$ (**8**) irreversibly. The photolysis of **3** in inert matrices (Ar, CH_4) demonstrates the occurrence of two pathways leading to (a) reversible loss of cyclopentadiene and formation of **7** and (b) oxidative hydrogen migration to form $ReCp(\eta^1\text{-}C_5H_5)(CO)_2H$ (**10**). Complex **10** is subject to secondary photolysis to yield first **5** and then **1** by sequential CO loss and ring coordination. The reactions of **3** in CO and N_2 matrices differ in two respects: (a) product **7** is replaced by **2** and **8**, respectively, and (b) **1** is subject to further photolysis to form **4**. Photolysis of **3** in ^{13}CO has been used to demonstrate that CO exchange with **3** is a very minor pathway. Complex **1** has been shown to react with CO in solution at room temperature to yield **3** and, in secondary reactions, **2**. The complete linkup in the matrix photochemistry of **1**, **2**, and **3**, together with their related solution photochemistry, leads to a mechanism for the solution addition of CO to **1** consisting of two CO addition steps with appropriate ring decoordination, followed by hydrogen transfer to give **2**. Evidence is presented that the hydrogen transfer takes place in a single step.

Introduction

In an earlier paper we reported on the photochemistry of MCp_2H_2 (M = Mo, W; Cp = η-C_5H_5) in low-temperature matrices and the characterization of the resulting metallocenes.[1,2] This paper is concerned with the matrix photochemistry of $ReCp_2H$ (**1**) and the related carbonyl complexes $ReCp(CO)_3$ (**2**) and $ReCp(\eta^2\text{-}C_5H_6)(CO)_2$ (**3**). Also included are photochemical reactions of **1** and **3** in solution in the presence of CO. Although the photosensitivity of MCp_2H_2 (M = Mo, W) is well established,[3] no photochemistry of the isoelectronic monohydride, **1**, or the trihydrides MCp_2H_3 (M = Nb, Ta) has been recorded previously. Our investigations show that all members of this group of molecules are indeed photosensitive.[4] The reaction of **1** with CO to form **3** was perhaps the earliest example of metal-to-ring hydrogen transfer,[5] yet the mechanism of this reaction remains unknown. Subsequently ring ⇌ metal hydrogen and alkyl transfers have been postulated frequently,[6-10] but it is rarely possible to observe each stage of the reaction. A notable exception is the recent demonstration of an alkyl transfer via carbonyl dissociation in Ar matrices.[11] Photochemical reactions of $ReCp(CO)_3$ (**2**) have been used on several occasions to synthesize substituted compounds,[12-14] $ReCp(CO)_2L$ and the dimer[15] $[ReCp(CO)_2]_2(\mu\text{-}CO)$. As expected for the intermediate $ReCp(CO)_2$, postulated by Foust et al.,[15] quantitative studies show that photosubstitution proceeds with a quantum yield of 0.30, independent of the concentration of the entering ligand.[14] The manganese analogue, $MnCp(CO)_3$, has been photolyzed in glasses[16] and noble-gas matrices,[17] yielding $MnCp(CO)_2$ reversibly, but in dinitrogen matrices $MnCp(CO)_2N_2$ is formed irreversibly.[17] In this paper we identify photochemical intermediates linking **1**, **2**, and **3**, enabling us to postulate a mechanism for the hydrogen-transfer reactions and to confirm the mechanism of subsitution of **2**. The validity of the proposed mechanism for solution reactions is supported by the photochemical reactions of **1** and **3** in solution. The results demonstrate the diversity of photochemical reactions of (cyclopentadienyl)metal hydrides and allow the characterization of the previously unknown metallocene $ReCp_2$ (**4**) by several spectroscopic methods. Some of these results have been reported in a preliminary communication.[18]

† No reprints available.

Experimental Section

The matrix-isolation equipment, absorption spectrometers, and photolysis lamps are described in a previous publication.[1] Laser-excited fluorescence spectra were induced with a CW argon ion laser (Spectra Physics 165) and analyzed with a Spex Ramalog 5 spectrometer using 90° collection from a canted CsI window. The excitation wavelengths were 514.5, 501.7, 496.5, 488.0, 476.5, 472.7, 465.8, andd 457.9 nm. The spectra were calibrated from the unwanted plasma lines, which were not filtered out. The photolysis radiation from the mercury arc was filtered with H_2O or $CoSO_4/NiSO_4$ solutions ($220 < \lambda < 340$ nm) or a Calflex C filter ($\lambda > 375$ nm). The UV/vis/near-IR experiments were carried out with a front-silvered mirror reflecting the photolysis radiation but with no water filter. The IR spectra of **2** and **3** (CH_4 matrix) were run with a Ge filter in the sample beam to prevent possible photolysis of the products by the Nernst glower. Matrix gases were from BOC (Research Grade) or BOC Prochem

(1) Chetwynd-Talbot, J.; Grebenik, P.; Perutz, R. N. *Inorg. Chem.* **1982**, *21*, 3647.
(2) Grebenik, P.; Downs, A. J.; Green, M. L. H.; Perutz, R. N. *J. Chem. Soc., Chem. Commun.* **1979**, 742.
(3) Berry, M.; Cooper, N. J.; Green, M. L. H.; Simpson, S. J. *J. Chem. Soc., Dalton Trans.* **1980**, 29. Berry, M.; Elmitt, K.; Green, M. L. H. *Ibid.* **1979**, 1950.
(4) The matrix photochemistry of MCp_2H_3 (M = Nb, Ta) will be reported separately.
(5) Fischer, E. O.; Wirzmüller, A. *Z. Naturforsch., B: Anorg. Chem., Org. Chem., Biochem., Biophys., Biol.* **1957**, *12B*, 737. Green, M. L. H.; Wilkinson G. *J. Chem. Soc.* **1958**, 4314.
(6) Müller, J.; Menig, H.; Rinze, P. V. *J. Organomet. Chem.* **1979**, *181*, 387.
(7) Whitesides, T. H.; Shelly, J. *J. Organomet. Chem.* **1975**, *92*, 215.
(8) Blackborow, J. W.; Eady, C. R.; Grevels, F. W.; Koerner von Gustorf, E. A.; Scrivanti, A.; Wolfbeis, O. S.; Benn, R.; Brauer, D. J.; Krüger, C.,; Roberts, P. J.; Tsay, Y. H. *J. Chem. Soc., Dalton Trans.* **1981**, 661.
(9) Benfield, F. W. S.; Green, M. L. H. *J. Chem. Soc., Dalton Trans.* **1974**, 1324.
(10) Humphries, A. P.; Knox, S. A. R. *J. Chem. Soc., Dalton Trans.* **1975**, 1711.
(11) Gerhartz, W.; Ellerhorst, G.; Dahler, P.; Eilbracht, P. *Liebigs Ann. Chem.* **1980**, 1296.
(12) Butler, I. S.; Cozak, D.; Stobart, S. R. *Inorg. Chem.* **1977**, *16*, 1779. Butler, I. S.; Cotville, N. J.; Cozak, D. *J. Organomet. Chem.* **1977**, *133*, 59.
(13) Sellman, D.; Kleinschmidt, E. *Z. Naturforsch., B: Anorg. Chem., Org. Chem.* **1977**, *32B*, 795. Sellman, D. *J. Organomet. Chem.* **1972**, *36*, C27.
(14) Giordano, P. J.; Wrighton, M. S. *Inorg. Chem.* **1977**, *16*, 160.
(15) Foust, A. S.; Hoyano, J. K.; Graham, W. A. G. *J. Organomet. Chem.* **1971**, *32*, C65.
(16) Braterman, P. S.; Black, J. D. *J. Organomet. Chem.* **1972**, *39*, C3.
(17) Rest, A. J.; Sodeau, J. R.; Taylor, D. J. *J. Chem. Soc., Dalton Trans.* **1978**, 651.
(18) Chetwynd-Talbot, J.; Grebenik, P.; Perutz, R. N. *J. Chem. Soc., Chem. Commun.* **1981**, 451.

0020-1669/83/1322-1675$01.50/0

Table II

Bands of **4** ($ReCp_2$) Generated from **1** ($ReCp_2H$) (cm^{-1})

IR: matrix; precursor				vis absorption: CO matrix; 1 precursor		vis emission:[a] CO matrix; 1 precursor					
CO; **1**	CO; **1**-*d*	N_2; **1**	CO; $Re(\eta\text{-}C_5D_5)_2H$	A[b]	B[b]	C[b]	diff	D[b]	diff	E[b]	diff
1102	1102	1102	1054, 1045	20 080	20 284	20 353	325	20 242	324	20 192	320
996	997	997	772	20 408	20 619	20 026	323	19 919	331	19 860	327
991			616	20 738	20 921	19 703	326	19 588	324	19 546	334
822	822	821, 818		21 097		19 378	320	19 264	332	19 211	338
317		316	305	21 473		19 057		18 933	336	18 877	332
299		298	289	21 820				18 600		18 544	

IR Bands of **5** ($ReCp(\eta^3\text{-}C_5H_5)(H)(CO)$) and HCO Generated from **1** (cm^{-1})

	^{12}CO; **1**	1% ^{12}CO/Ar; **1**	^{12}CO; **1**-*d*	$^{12}CO/^{13}CO$ (1:1); **1**	^{13}CO; **1**-*d*	^{12}CO; $Re(\eta\text{-}C_5D_5)_2H$
5	1918	1929	1921	1918/1872.5	1873.5	1919
HCO	2488		2486			2488
HCO	1860	1860	1860	1860/1820	1821	1860
HCO	1091		1090		1085	1091
DCO			1800		1780	

[a] The emission bands are listed as averages of all observations for up to seven excitation wavelengths. The differences are averaged from each observation of pairs of adjacent bands. The absolute frequencies varied by 18–25 cm^{-1} according to the excitation wavelength. [b] A-E are the progressions discussed in the text.

(^{13}CO, 97 atom %; $^{15}N_2$, 99 atom %).

The precursor, **1**, was prepared by the reaction of $ReCl_5$, NaCp, and $NaBH_4$.[19] The product was recrystallized from toluene and sublimed prior to use. $ReCp_2D$, **1**-*d*, was prepared by treating **1** with dilute DCl followed by precipitation with NaOD. $Re(\eta\text{-}C_5D_5)_2H$ was prepared from NaC_5D_5 in the same manner as **1**. NaC_5D_5 was synthesized by reaction of cyclopentadiene-d_6 (prepared as in ref 20) with sodium sand in THF. The isotopic purity of the $Re(\eta\text{-}C_5D_5)_2H$ was estimated at ca. 90% by mass spectrometry.

The precursor, **2**, was synthesized by reaction of $Re_2(CO)_{10}$ (Strem) with chlorine[21] to form $Re(CO)_5Cl$ followed by reaction[22] with NaCp. It was purified by sublimation and identified by IR and mass spectrometry.

The hydride, **1**, was carbonylated to form **3** with low pressures of CO rather than the published method.[5] **1** (0.3 g, 0.9 mmol) was dissolved in petroleum ether (bp 100–120 °C) (10 cm^3) in a 50-cm^3 ampule pressurized with 1 atm CO, and was heated at 120 °C for 2 days (protected by a blast tube). The reaction was monitored by IR spectroscopy of the solution, which showed that the major product was **3** (ν_{CO} = 1973, 1904 cm^{-1}) with traces of **2** also present (ν_{CO} = 2025, 1939 cm^{-1}). The product was separated from residual **1** by extraction of **1** with dilute HCl and was purified by sublimation. It was identified by IR, NMR, and mass spectrometry. The carbonylation of **1** was also carried out photochemically in cyclohexane solution in a Pyrex vessel ($\lambda > 285$ nm) with CO at 1 atm. In both thermal and photochemical experiments the ampule was replenished with CO each time that a sample was withdrawn for IR spectroscopy.

The samples were sublimed into the matrices at the following temperatures: **1**, 310–323 K; **2**, 268–273 K; **3**, 322–333 K. The substrate was maintained at 17–20 K during deposition, and the matrix gases were deposited at 1–3 mmol h^{-1} for ca. 1 (**2**) or 2–4 h (**1** and **3**).

Results

$ReCp_2H$ (1) in Matrices. The IR spectrum of **1** and its deuterated analogues will be discussed in detail elsewhere.[23] Here we list the wavenumbers of **1** (Table I, supplementary material)[24] and note the weak, broad Re–H stretching mode at 2032 cm^{-1} (CO) and the more conspicuous sharper Re–H deformation modes at 846 and 515 cm^{-1}, which are shifted to 1448, 640, and 457 cm^{-1}, respectively in $ReCp_2D$, **1**-*d*. Although no photolysis products were detected in Ar matrices,

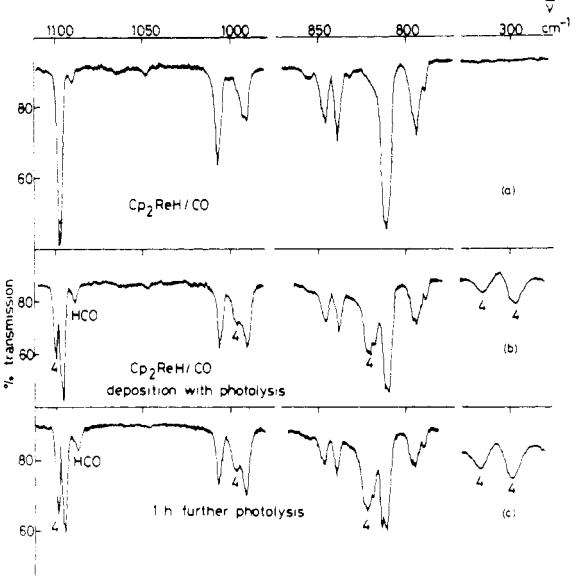

Figure 1. IR spectra of **1** ($ReCp_2H$) below 1150 cm^{-1}: (a) spectrum following codeposition with CO at 17 K (4-h spray-on, sublimation temperature 310 K, 2.4 mmol of CO); (b) spectrum following codeposition with CO at 17 K with simultaneous unfiltered UV photolysis (3.3-h spray-on at 310 K, 2.2 mmol of CO) showing bands of **4** ($ReCp_2$); (c) same as (b) but with 1 h further UV photolysis showing further growth of **4**.

products were observed in CO or N_2 matrices and in Ar doped with CO and N_2. On photolysis in solid CO (314 nm or unfiltered Hg arc, 1–3 h) the bands of **1** decreased in intensity and several new bands were detected in the 1150–250-cm^{-1} region (Figure 1, Table II). These bands maintained a constant intensity ratio independent of photolysis time. They were generated in increased yield by using simultaneous photolysis and deposition, reaching a maximum conversion of ca. 50%. The yield was reduced in an Ar/CO (1:1) matrix, and they were no longer detected in matrices containing <20% CO. With the exception of a product band at 1091 cm^{-1} (assigned to HCO; see below), a similar set of bands was generated on photolysis in solid dinitrogen. They are assigned to a single noncarbonyl product, **4**.

A UV/vis/near-IR experiment in solid CO showed an intense absorption of **1** at 250 nm with shoulders at 280 and 330 nm. When the 2600–300-nm range was scanned after pho-

(19) Green, M. L. H.; Pratt, L.; Wilkinson, G. *J. Chem. Soc.* **1958**, 3916.
(20) Gallinella, E.; Mirone, P. *J. Labelled Compd.* **1971**, *7*, 183.
(21) Abel, E. W.; Wilkinson, G. *J. Chem. Soc.* **1959**, 1501.
(22) Hammond, G. S.; Leermakers, P. A.; Turro, N. J. *J. Am. Chem. Soc.* **1961**, *83*, 2396.
(23) Grebenik, P.; Perutz, R. N., to be submitted for publication.
(24) See paragraph at end of the paper regarding supplementary material.

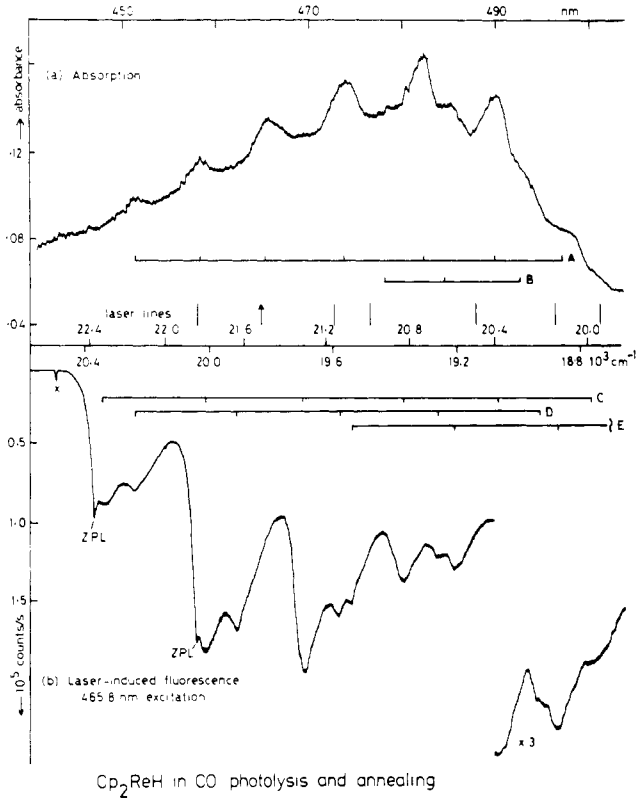

Figure 2. (a) Visible absorption spectrum of **4** ($ReCp_2$) obtained on 70-min deposition of **1** ($ReCp_2H$, sublimed at 310 K) with CO (3.6 mmol) at 20 K; 20-min subsequent Hg arc photolysis ($220 < \lambda < 340$ nm); subsequent annealing at 37 K and recooling to 20 K; slit 0.8 nm (~35 cm^{-1}). (b) Laser-excited fluorescence of **4** obtained on 95-min codeposition of **1** (sublimed at 313 K) with CO (3.3 mmol) at 20 K; 30-min subsequent Hg arc photolysis ($220 < \lambda < 340$ nm); subsequent annealing to 37 K and recooling to 18 K; laser excitation at 465.8 nm (arrow in part a), power 75 mW, spectrometer slit 4.5 cm^{-1}, × = plasma line of laser. ZPL = zero phonon line. Note that the wavenumber scales differ from those in part a.

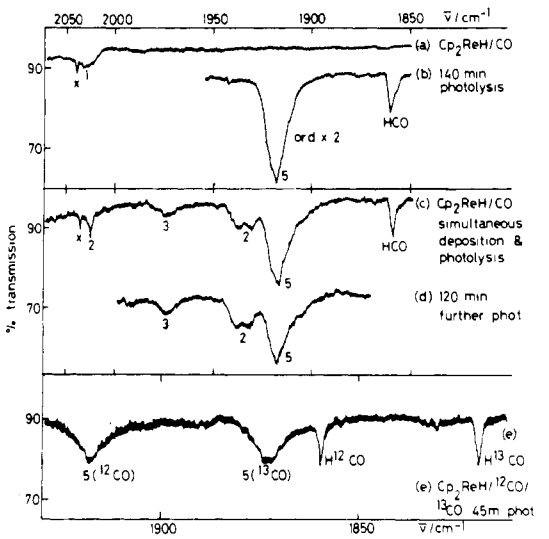

Figure 3. IR spectra in the carbonyl and metal–hydride stretching region: (a) spectrum following codeposition of **1** ($ReCp_2H$) with CO at 17 K (same experiment as in Figure 1a); (b) spectrum after 140-min subsequent unfiltered UV photolysis; (c) spectrum following codeposition of **1** with CO at 17 K with simultaneous unfiltered UV photolysis (same experiment as in Figure 1b); (d) same as (c) but with 120 min further UV photolysis; (e) spectrum following codeposition of **1** with $^{12}CO/^{13}CO$ (1:1) at 20 K (1-h spray-on at 323 K, 3.4 mmol of CO) and 45-min subsequent unfiltered UV photolysis. The numbering of the products is as in the text. × = impurity.

tolysis, one highly structured product absorption was detected, which sharpened considerably on annealing (Figure 2, Table II). The major vibrational progression, A, had seven members with a mean separation of 347 cm^{-1}; a second progression, B, of three members with mean separation 318 cm^{-1} could also be discerned. The considerable reduction in intensity in an Ar/CO (9:1) matrix and the strong vibrational structure lead us to assign this band to **4**. (The high intensity of the visible absorption makes this a more sensitive method of detecting **4** than IR spectroscopy, so explaining the lack of **4** in IR spectra of matrices containing <20% CO.)

The convenient position of this visible absorption allowed us to look for laser-excited fluorescence (LEF). After a photolyzed sample of **1** in CO was annealed, an intense structured emission spectrum was found with excitation by any of seven lines of the Ar^+ laser between 501.7 and 457.9 nm but not with 514.5 nm excitation, which lies just outside the absorption envelope (Figure 2, Table II). The emission peaks showed a sharp onset at 20 360 cm^{-1} (unless $\nu_{ex} < 20\,360$ cm^{-1}) and were grouped into three progressions (C, D, E) with a progression frequency of 324–330 cm^{-1}. Progression C was observed with all excitation wavelengths except 501.7 nm, and progression D with all except 476.5 nm. In these progressions, the second and third members were always the most intense. Progression E was intense with 501.7-nm excitation but was weak otherwise. The frequencies of the progression intervals varied by <14 cm^{-1} with different excitation wavelengths and are listed in Table II as an average for all observations of adjacent bands. In addition to these bands, zero phonon lines (see e.g. ref 25a) were observed with 465.8-nm (Figure 2) and 501.7-nm excitation. Together these features account for all bands out to 1500 cm^{-1} from the onset of fluorescence with the exception of some unique features observed on irradiating into the tail of the absorption at 501.7 nm. The match of the excitation profile of the LEF spectrum and the progression frequencies with the absorption spectra leave no doubt that the emission must be assigned to **4**.

In addition to the bands of **4**, several IR bands were observed in the carbonyl region on photolysis of **1** in solid CO (Figure 3). The sharp band at 1860 cm^{-1} correlated with **4** and may be assigned together with weaker bands at 2488 and 1091 cm^{-1} to HCO.[25b] Prolonged photolysis reduced the yield of HCO. The most intense band in the carbonyl region (1918 cm^{-1}) was generated in greatest yield in a Ar/CO (4:1) matrix and was still detected in a Ar/CO (100:1) matrix. These dilution experiments suggest that this product, **5**, is a monocarbonyl. On prolonged photolysis in CO matrices, but not in Ar/CO mixed matrices, further carbonyl bands were generated at the expense of **5**. These bands at 2028, 1939, and 1934 cm^{-1} are within 3 cm^{-1} of those observed for **2** isolated in a CO matrix (see Table I). An additional weak band at 1975 cm^{-1} is only 4 cm^{-1} to high frequency of the band of **3** in a CO matrix (the second band of **3** would be obscured by the tail of the absorption of **5**). On photolysis of **1** in solid dinitrogen, one band is generated in the N–N stretching region at 2125 cm^{-1} assigned to a product **6**. Further information concerning the nature of **4**, **5**, and **6** was obtained by isotopic subsitution.

On photolysis of **1-*d*** in a CO matrix, the four most intense bands of **4** were detected unshifted, indicating that **4** does not contain the hydridic hydrogen. However the CO stretching band of **5** was shifted 3 cm^{-1} to high frequency (Table II). This is readily explained as a consequence of interaction between the Re–H and C–O stretching fundamentals in a rhenium hydride carbonyl (cf. the behavior of $HRe(CO)_5$/$DRe(CO)_5$).[26] Surprisingly HCO was detected considerably

(25) (a) Brus, L. E.; Bondybey, V. E. *J. Chem. Phys.* **1975**, *63*, 3123. (b) Milligan, D. E.; Jacox, M. E. *Ibid.* **1964**, *41*, 3032; **1969**, *51*, 277.

Table III. Wavenumbers of the Photoproducts of $ReCp(CO)_3$ (2) and of Related Manganese Compounds[a] (cm^{-1})

$ReCp(CO)_2$ (7) Ar matrix	$ReCp(CO)_2N_2$ (8) N_2 matrix	$MnCp(CO)_2$ Ar matrix	$MnCp(CO)_2N_2$ N_2 matrix
1963	2152	1972	1975.3
1961	2146		
1897.5	1973	1903.2	1978.7
1895	1919		1927

[a] Data for Mn compounds are from ref 17.

more strongly than DCO (Table II). The possibility of exchange between ring hydrogen atoms and deuterium was excluded by checking for growth of the Re–H deformation modes of **1**.

The effect of deuteration was investigated further by photolyzing $Re(\eta\text{-}C_5D_5)_2H$ in CO. The bands of **4** were shifted substantially (Table II) whereas the CO stretching bands of the products **5**, **2**, and **3** were <1 cm^{-1} from their positions in experiments with **1**. Again HCO was observed, but no trace of DCO could be detected even at high ordinate expansion.

The nature of **5** was clarified by conducting an experiment in a $^{12}CO/^{13}CO$ (1:1) matrix (Figure 3e). The carbonyl region of the spectrum shows four bands after a 45-min photolysis, which are assigned to $H^{12}CO$, $H^{13}CO$, **5** (^{12}CO), and **5** (^{13}CO) (Table II). The absence of any bands in the region between **5** (^{12}CO) and **5** (^{13}CO) confirms that **5** is a monocarbonyl. Photolysis of **1**-*d* in ^{13}CO results in production of **5** (^{13}CO), $H^{13}CO$, and traces of $D^{13}CO$.

The possibility that **6** is a dinitrogen complex was tested by using a $^{15}N_2/^{14}N_2$ (1:1) matrix. In addition to the band at 2125 cm^{-1}, a product band was detected at 2054 cm^{-1}, within 1 cm^{-1} of the position predicted on the basis of the reduced mass ratios of $^{15}N_2$ and $^{14}N_2$.

These experiments provide sufficient information to assign structures for **4**, **5**, and **6**. There are several grounds for assigning **4** as rhenocene, $ReCp_2$: (a) it is generated in both CO and N_2 matrices and so cannot contain any coordinated CO; (b) it is associated with the production of HCO in CO matrices; (c) its IR spectrum is unaffected by deuteration of the hydridic hydrogen but is strongly affected by deuteration of the ring hydrogens; (d) its IR spectrum is remarkably similar to those of other metallocenes, and its bands shift similarly on deuteration (see Table of ref 18);[1,27] (e) it shows a highly structured visible absorption comparable with the spectra of $MoCp_2$, WCp_2, $FeCp_2$, and $[FeCp_2]^+$;[1,28,29] (f) on laser excitation in the visible absorption band, a structured emission is observed (cf. phosphorescence of $FeCp_2$).[28] The first carbonyl product, **5**, has been shown by isotopic substitution to be a hydrido monocarbonyl and is assigned as $ReCp(\eta^3\text{-}C_5H_5)(H)(CO)$ on the basis of the 18-e rule (cf. $WCp(\eta^3\text{-}C_5H_5)(CO)_2$).[30] We consider that the isomer $ReCp(\eta^4\text{-}C_5H_6)CO$ is inconsistent with the data. The product **6** found in dinitrogen matrices has been shown to be a mono(dinitrogen) complex and is assigned as $ReCp(\eta^3\text{-}C_5H_5)H(N_2)$ by analogy with **5**.

The effect of dilution strongly suggests that there are two independent photochemical pathways for **1**: (1) hydrogen loss, which is associated with CO capture to form HCO in a CO matrix, or (2) CO or N_2 addition, which is followed by secondary photolysis to give polycarbonyls. The problem of reconciling the isotopic data on HCO is postponed to the Discussion.

The photochemistry of **1** in matrices is summarized in eq 1–3.

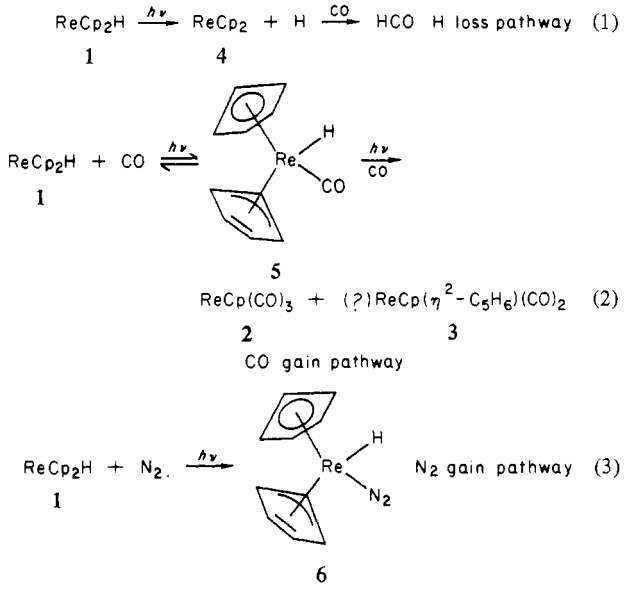

$ReCp(CO)_3$ (2) in Matrices. The photochemistry of **2** was investigated in Ar, N_2, and CO matrices. As is common for matrix spectra[17] of such compounds, the CO stretching bands were split into several components because of trapping in multiple sites (Table I). On photolysis in Ar the two CO stretching fundamentals decreased by ca. 25% after 6-min UV ($220 < \lambda < 340$ nm) photolysis and two product bands grew to lower wavenumbers; a weak band assigned to CO was observed at 2138 cm^{-1}. The new bands, assigned to product **7**, were bleached completely by visible radiation (10 min, $\lambda > 375$ nm), and the precursor **2** was regenerated (Table III). The release of CO, the ready reversibility of the generation of **7**, and the analogy[17] with $MnCp(CO)_3$ and many other metal carbonyls that have been investigated in matrices[31] leave no doubt that **7** is the unsaturated species $ReCp(CO)_2$.

The photochemistry of **2** in N_2 matrices was investigated by using a particularly high dilution (sublimation temperature 268 K; deposition with 4 mmol of N_2 in 1 h). The initial photoproducts included CO (2139 cm^{-1}) and three bands (Table III) within 5 cm^{-1} of the bands reported for $ReCp(CO)_2N_2$ (**8**) in hexane solution (2141, 1970, 1915 cm^{-1}).[13] This reaction was not reversed by visible irradiation, but further UV photolysis caused secondary reactions to give products with several bands in the 2150–1900-cm^{-1} region. The details of these secondary reactions will be reported elsewhere. At higher concentrations evidence of dimeric species was found on prolonged photolysis, as shown by absorptions in the 1750–1850-cm^{-1} region. In CO matrices **2** did not show photosensitivity.

The matrix photochemistry of **2** is summarized by eq 4 and 5.

$$\underset{\mathbf{2}}{ReCp(CO)_3} \underset{\text{vis, Ar}}{\overset{\text{UV, Ar}}{\rightleftharpoons}} \underset{\mathbf{7}}{ReCp(CO)_2} + CO \qquad (4)$$

$$ReCp(CO)_3 \xrightarrow[-CO]{\text{UV, } N_2} \underset{\mathbf{8}}{ReCp(CO)_2N_2} \xrightarrow[N_2]{\text{UV}} \text{secondary products} \qquad (5)$$

$ReCp(\eta^2\text{-}C_5H_6)(CO)_2$ (3) in Matrices. The photochemistry of **3** was examined in Ar, CH_4, CO, and N_2 matrices. In all

(26) Braterman, P. S.; Harrill, R. W.; Kaesz, H. D. *J. Am. Chem. Soc.* **1967**, *89*, 2881.
(27) Lippincott, E. R.; Nelson, R. D. *Spectrochim. Acta* **1958**, *10*, 307.
(28) Smith, J. J.; Meyer, B. *J. Chem. Phys.* **1968**, *48*, 5436.
(29) Hendrickson, D. N.; Sohn, Y. S.; Duggan, D. M.; Gray, H. B. *J. Chem. Phys.* **1973**, *58*, 4666.
(30) Huttner, G.; Brintzinger, H. H.; Bell, L. G.; Friedrich, P.; Bejenke, V.; Neugebauer, D. *J. Organomet. Chem.* **1978**, *145*, 329.
(31) Perutz, R. N.; Turner, J. J. *J. Am. Chem. Soc.* **1975**, *97*, 4791. Poliakoff, M.; Turner, J. J. *J. Chem. Soc., Dalton Trans.* **1973**, 1351.

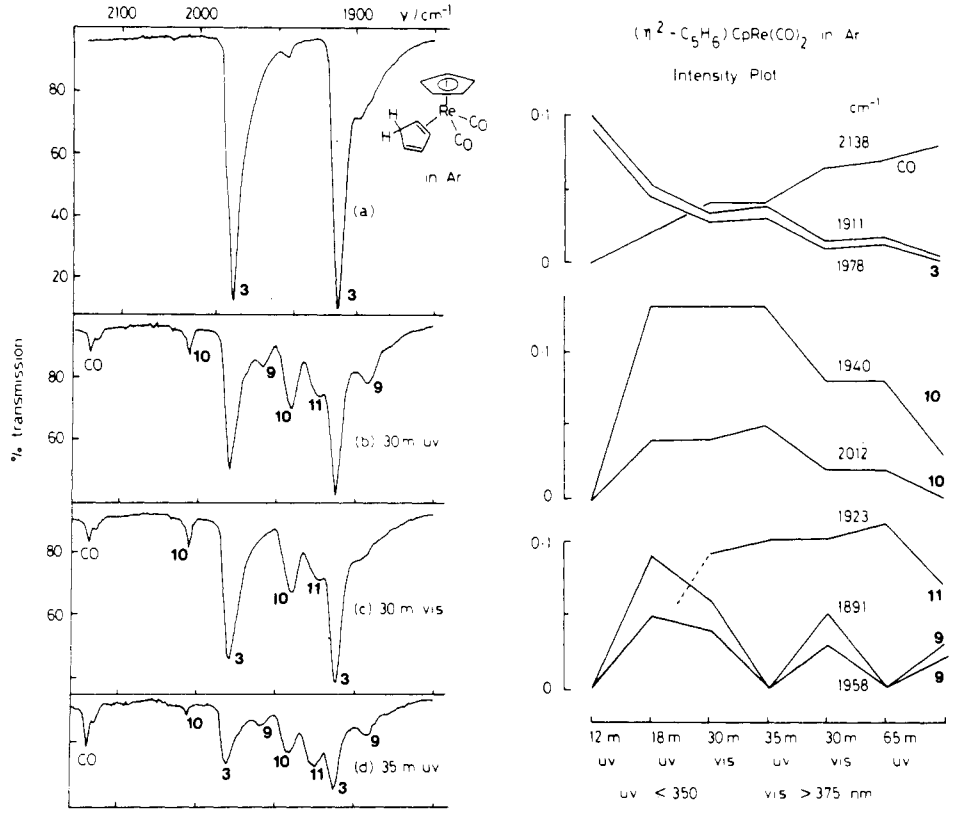

Figure 4. Left: (a) IR spectrum of **2** ($ReCp(\eta^2\text{-}C_5H_6)(CO)_2$) in Ar at 14 K (2-h spray-on at 322 K, 1.5 mmol of Ar) showing the CO stretching region; (b) spectrum after 30-min UV photolysis ($220 < \lambda < 340$ nm); (c) spectrum after 30-min visible photolysis ($\lambda < 375$ nm); (d) spectrum after 35-min further UV photolysis as in (b). The products are labeled as in the text. Right: Intensity plot for all photolysis stages of the experiment showing the different behavior of products **9**, **10**, and **11**.

four matrices **3** showed two CO stretching bands of similar intensity at ca. 1975 and ca. 1905 cm^{-1}, which were appreciably broader than those of **2**. The complete set of IR bands of **3** is listed in Table I. The bands of **3** decreased by ca. 50% after 12-min UV photolysis ($220 < \lambda < 340$ nm), and after 165 min 95% of **3** had been photolyzed. In methane matrices the reactions proved faster (as is found for many metal carbonyls), and the photolysis of **3** was 90% complete after 45 min. In both matrices there were five product absorptions in the CO stretching region in addition to free CO. From a plot of their optical densities as a function of photolysis time, it was apparent that they belong to the three products **9**, **10**, and **11** (Figure 4). Product **9**, with two bands to lower wavenumbers than those of **3**, grows during the first 5–10 min of UV photolysis but is almost wholly destroyed by longer wavelength photolysis ($\lambda > 375$ nm). After long-wavelength photolysis, the absorbance of **3** was found to have increased but no change was detected in the absorbance of free CO. Further UV photolysis caused an initial recovery of **9**, but subsequently **9** decreased in secondary photochemical reactions. Product **10**, with two bands to higher wavenumbers than those of **3**, grows at a rate similar to that of **9** in the initial stages of photolysis and is also destroyed by prolonged photolysis. However, it is distinguished from **9** by its behavior on long-wavelength photolysis; in Ar matrices it is unaffected, and in CH_4 matrices it increases slightly.[32a] Product **11** shows one CO stretching band (ca. 1920 cm^{-1}) that becomes apparent only when **9** and **10** are decreasing during secondary photolysis. Measurement of its absorbance is hampered by overlap with **3**, but it appears to increase marginally on long-wavelength photolysis in Ar. Prolonged photolysis eventually destroys **11** in addition to **9** and **10**.

After 2–4-h UV photolysis the bands in the CO stretching region are all very weak. At this stage examination of the IR spectrum below 1450 cm^{-1} revealed all the medium- and high-intensity bands of **1**. Some of its weaker bands were also observed together with the four most intense bands of cyclopentadiene (Ar matrices, Table IV), which were identified by comparison with the matrix spectra of an authentic sample (Table I).

The effect of dilution in Ar matrices was examined by using an 8-fold excess of matrix gas compared to our usual experimental conditions. The bands of **3** were shown to be unaffected by longer wavelength photolysis ($\lambda > 375$ nm) but were somewhat more photosensitive when irradiated with UV light (ca. 50% decrease in intensity was observed after a 4-min photolysis). Product bands due to **9** and **10** appeared after a short period of photolysis and behaved similarly to our previous observations, although some additional splittings were evident. Visible photolysis converted **9** mainly to **3**, but as in CH_4 matrices, a small increase in the amount of **10** was noted. On further photolysis, **11** was formed.

The photochemistry of **3** in N_2 matrices differed from that in Ar and CH_4 matrices in one important respect: product **9** was absent, and instead a product was observed at 2150 cm^{-1} together with shoulders on the bands of **3** at 1972 and 1916 cm^{-1}. This product may be assigned to $ReCp(CO)_2N_2$ (**8**) by comparison with the matrix experiments on **2** and solution IR data on **8**.[13] The products **10**, **11**, and **1** were observed as before, but cyclopentadiene was absent. As expected, considering the photochemistry of **1** in N_2 matrices, there was some evidence for formation of **4**.

(32) (a) During photolysis in methane matrices, the CO stretching band developed shoulders 4–5 cm^{-1} to low frequency. These may be attributed to regeneration of **3** from **9** in a different conformer, formed by rotation of the cyclopentadienyl ligand. (b) Perturbation of the IR spectrum of photoproducts by expelled ligands in matrices is well documented.[1,31] In the case of WCp_2 interaction was observed with CO when generated from WCp_2CO and with ethene when generated from $WCp_2(C_2H_4)$.

Table IV. Wavenumbers of Photoproducts of $ReCp(\eta^2\text{-}C_5H_6)(CO)_2$ (3) in Matrices (cm^{-1})

$ReCp_2H$ (1)				$ReCp(CO)_2$ (9 (=7))		$ReCp(\eta^1\text{-}C_5H_5)(H)(CO)_2$ (10)				$ReCp(CO)_3$ (2) CO
Ar[c]	CH_4[c]	N_2[c]	CO[c]	Ar	CH_4	Ar	CH_4	N_2	CO	
1420	*a*	1420	1420	1959	1949	2013	2008	2011	2008	2029
1400	*a*	1402	1399	1893	1880	1942	1931	1938	*a*	1933
1344	*a*	1345	1344							615
1099	1099	1099	1098							610 (sh)
1007	1007	1008	1008							600
990	991	992	992							515
844	845	847	842							507
836	838	838	—							
807	809	810	811							
789	793	793	795							
587	*a*	588	588							
502	*a*									
420	*a*	420	420							
	a	394								
357	*a*	356								

C_5H_6		$ReCp(\eta^3\text{-}C_5H_5)(H)(CO)$ (11 (=5))				$ReCp(CO)_2N_2$ (8) N_2	$ReCp_2$ (4)	
Ar[c]	CO[c]	Ar	CH_4	N_2	CO		N_2	CO
1369	1368	1923	1914	1923	1918 (sh)	2150	1102 (sh)	1102
966	962					1972 (sh)		998
894	894					1916 (sh)	819 (sh)	822
670	672							
	775[b]							
	725[b]							

[a] Obscured. [b] Photoproduct of C_5H_6. [c] Matrix throughout.

When **3** was irradiated in CO matrices, the most conspicuous carbonyl product had absorptions at 2029 and 1933 cm^{-1}; unlike the products in Ar and CH_4 matrices, this product was not subject to secondary photolysis. The agreement of intensity ratios, the positions of the CO stretching bands (compare Tables I and IV), and its photostability leave little doubt that this product is $ReCp(CO)_3$ (**2**). The slight discrepancies in the frequencies (1.5 cm^{-1} in $\nu_{CO}(a_1)$ and 7 cm^{-1} in $\nu_{CO}(e)$) may be explained by interaction with expelled cyclopentadiene[32b] (see below). Of the other carbonyl products, **9** is absent, but **10** and **11** are observed (one band of **10** overlaps **2**). In the low-frequency region the products **1**, **2**, **4**, and C_5H_6 were observed (compare Tables I and IV) together with a photolysis product of C_5H_6.

In a direct test of the postulate of interaction of **2** with cyclopentadiene when generated by photolysis of **3** in CO matrices, we isolated **2** in an Ar matrix containing 2% cyclopentadiene. The high-frequency CO stretching band (a_1) was found to be a doublet with a broad component at 2032 cm^{-1} in addition to the usual band at 2035.5 cm^{-1}. The low-frequency CO stretching mode (e) was broadened and exhibited an additional shoulder at ca. 1940 cm^{-1}, 5 cm^{-1} to low frequency of the main peak. These observations confirm that interaction between **2** and cyclopentadiene shifts the CO stretching bands of **2** in accord with the photochemical results on **3**.

Further information was obtained by photolyzing **3** in a pure ^{13}CO matrix. Visible photolysis ($\lambda > 375$ nm) had no effect on the absorptions of **3**. However, after 30-s UV photolysis, the bands of the starting material had decreased by ~15% and product bands had appeared at 2016 and 1934 cm^{-1}, which may be assigned to $ReCp(^{12}CO)_2(^{13}CO)$.[33] Surprisingly, there was no evidence for formation of any $ReCp(\eta^2\text{-}C_5H_6)(^{12}CO)(^{13}CO)$, whose absorptions should have been clearly detectable. A 5-min UV photolysis led to the appearance of bands at 2002, 1917, and 1895 (shoulder) cm^{-1} assigned to $ReCp(^{12}CO)(^{13}CO)_2$, a band at 2009 cm^{-1} (the high-frequency band of **10**), and weak features at 1953 and 1876 cm^{-1} assigned to a small percentage of $ReCp(\eta^2\text{-}C_5H_6)(^{12}CO)(^{13}CO)$.[33] The experiment confirms that the main carbonyl-containing product formed from **3** in CO matrices is $ReCp(CO)_3$ and demonstrates that CO loss from **3** is a very minor photochemical pathway compared to loss of C_5H_6.

We are now in a position to identify the photoproducts of **3**: **9**–**11**. The product **9** with its two bands to low frequency of **3** is converted back to its precursor on visible irradiation like many coordinatively unsaturated metal carbonyls.[17,31] Consistent with a dicarbonyl, the absorption of free CO does not decrease when **9** is reconverted to **3**. Product **9** is replaced in N_2 and CO by **8** and **2**, respectively, indicating that the "expelled ligand" is cyclopentadiene and that **9** = **7**, viz. $ReCp(CO)_2$. The slight discrepancy (4–5 cm^{-1}) between the bands of $ReCp(CO)_2$ when generated from **2** and **3** may be attributed to interaction with expelled C_5H_6 or CO[32b] (cf. the effect of interaction of C_5H_6 with **2**).

Product **10** must also be a dicarbonyl since it shows two CO stretching bands, but these are shifted to higher wavenumbers than those of **3**, indicating an oxidized species. It is unaffected by visible irradiation or the presence of CO or of N_2, suggesting coordinative saturation. Assuming the 18-e rule, we assign **10** as $ReCp(\eta^1\text{-}C_5H_5)H(CO)_2$.

Product **11** shows only one CO stretching band and, like **10**, shows the characteristics of coordinative saturation. Since **11** must be the monocarbonyl intermediate between **2** and **10** on the one hand and **1** on the other hand, we should expect a close relation to the product **5** obtained by CO addition to **1**. Indeed **5** absorbs at 1929 cm^{-1} when generated from **1** in 1% CO/Ar whereas **11** absorbs at 1923 cm^{-1} when formed from **3** in Ar. We conclude that **5** and **11** are identical, viz. $ReCp(\eta^3\text{-}C_5H_5)(H)(CO)$, and that the 6-$cm^{-1}$ discrepancy is due to interaction of **11** with expelled CO.[32b] Consistent with this, the absorption of **5** in solid CO is at 1918 cm^{-1} and is

(33) The frequencies of ^{13}CO-substituted carbonyls were calculated by standard energy-factored force constant methods. The resulting calculated frequencies were as follows (cm^{-1}). For **2** (using k = 1561.2 N m^{-1}, i = 49.3 N m^{-1}): $ReCp(^{12}CO)_3$, 2027.4, 1934.9; $ReCp(^{12}CO)_2(^{13}CO)$, 2016.2, 1934.9, 1902.2; $ReCp(^{12}CO)(^{13}CO)_2$, 2002.5, 1915.2, 1891.7. For **3** (assuming local C_s symmetry and k = 1515.3 N m^{-1}, i = 52.55 N m^{-1}): $ReCp(\eta^2\text{-}C_5H_6)(^{12}CO)_2$, 1970.4, 1903.2; $ReCp(\eta^2\text{-}C_5H_6)(^{12}CO)(^{13}CO)$, 1954.8, 1875.6; $ReCp(\eta^2\text{-}C_5H_6)(^{13}CO)_2$, 1926.5, 1860.8.

Scheme I

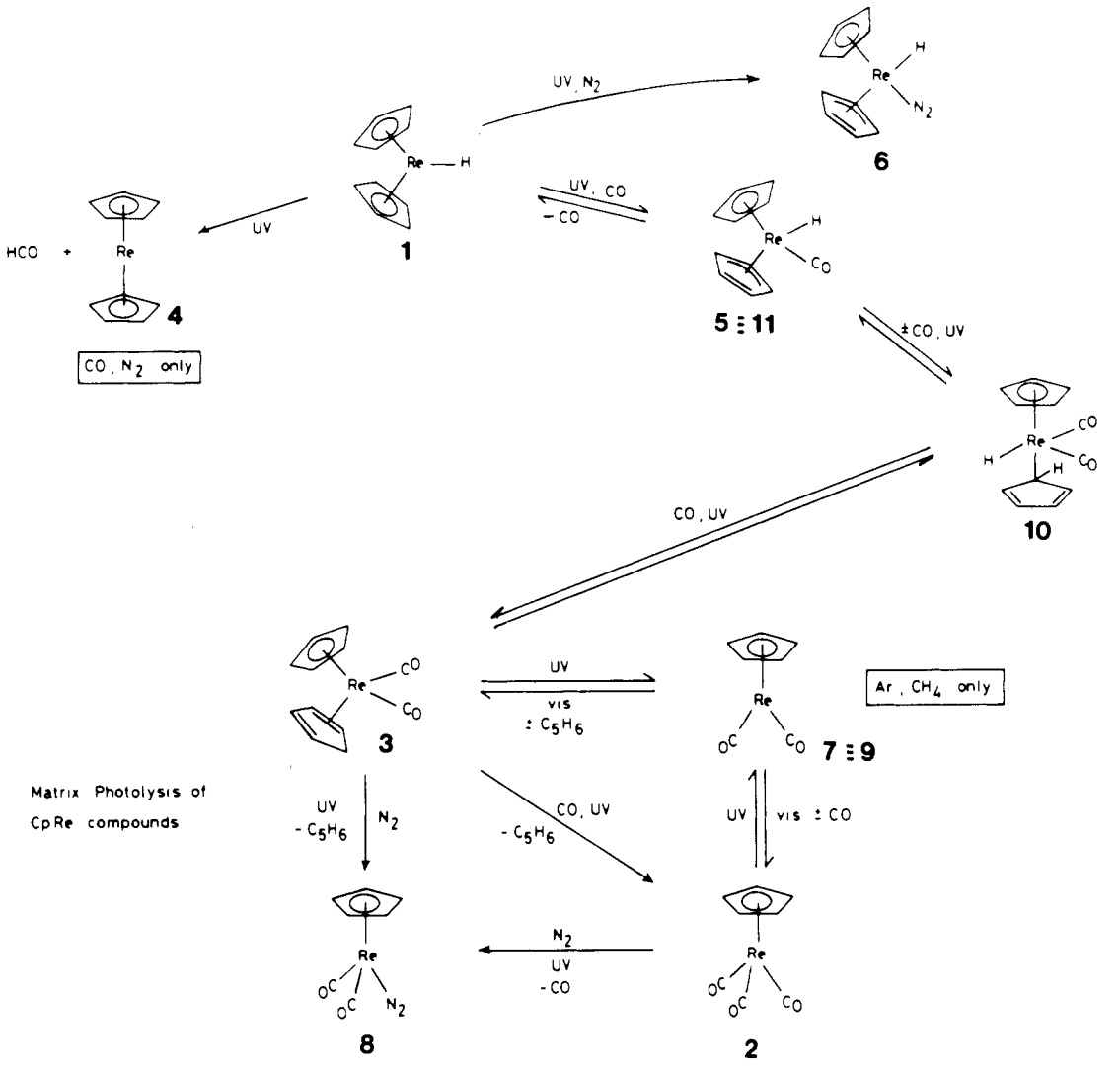

seen at the same frequency (as a shoulder) on photolysis of **3** in CO.

We may now summarize the matrix photochemistry of **3** by eq 6–11.

$$\underset{\mathbf{3}}{ReCp(\eta^2\text{-}C_5H_6)(CO)_2} \underset{\text{vis}}{\overset{\text{Ar, CH}_4\text{, UV}}{\rightleftharpoons}} \underset{\mathbf{9 = 7}}{ReCp(CO)_2} + C_5H_6 \quad (6)$$

$$3 \xrightarrow{N_2\text{, UV}} \underset{\mathbf{8}}{ReCp(CO)_2N_2} + C_5H_6 \quad (7)$$

$$3 \xrightarrow{\text{CO, UV}} \underset{\mathbf{2}}{ReCp(CO)_3} + C_5H_6 \quad (8)$$

$$3 \underset{N_2\text{, CO}}{\overset{\text{UV, Ar, CH}_4}{\rightleftharpoons}} \underset{\mathbf{10}}{ReCp(\eta^1\text{-}C_5H_5)(H)(CO)_2} \xrightarrow[-CO]{UV} \underset{\mathbf{11 = 5}}{ReCp(\eta^3\text{-}C_5H_5)(H)(CO)} \quad (9)$$

$$\underset{\mathbf{9}}{ReCp(CO)_2} + C_5H_6 \xrightarrow[\text{minor pathway}]{\text{Ar, CH}_4\text{, UV}} \underset{\mathbf{10}}{ReCp(\eta^1\text{-}C_5H_5)(H)(CO)_2} \quad (10)$$

$$\mathbf{11} \xrightarrow[-CO]{UV} \underset{\mathbf{1}}{ReCp_2H} \xrightarrow[UV]{\text{CO, N}_2\text{ only}} \underset{\mathbf{4}}{ReCp_2} \quad (11)$$

$ReCp_2H$ (1) in Solution. The photochemistry of **1** was studied in cyclohexane solution under 1 atm of CO with Pyrex-filtered radiation. After 6-h photolysis both **2** and **3** had been formed in substantial quantities. Further photolysis caused the bands of **2** to increase at the expense of **3**. After prolonged photolysis some weaker IR bands were detected, which remained unassigned. No bands were detected that could be assigned to a monocarbonyl intermediate between **1** and **3**. These observations are consistent with the reaction sequence:

$$\underset{\mathbf{1}}{ReCp_2H} \xrightarrow[CO]{h\nu} \underset{\mathbf{3}}{ReCp(\eta^2\text{-}C_5H_6)(CO)_2} \xrightarrow[CO]{h\nu} \underset{\mathbf{2}}{ReCp(CO)_3} + C_5H_6$$

1977, 1908 cm^{-1} 2028, 1944 cm^{-1}

Discussion

The photochemical reactions in matrices of **1** and **3** are summarized in Scheme I, which illustrates how the chemistry of the three complexes is linked through the common intermediates **5**, **7**, and **10**. These observations lead to an intimate mechanism for the hydrogen migration step and have also defined new photochemical pathways for the metal hydrides **1**, **5**, and **10**. Meanwhile, the solution reactions of **1** suggest that the mechanistic conclusions are valid not only in matrices but also in solution.

Photochemical Pathways from 1 in Matrices. The photochemical reactions of metal polyhydrides are dominated by reductive elimination of H_2, but occasionally displacement of

other ligands is observed instead.[1,34] A variety of reactions has been observed on photolysis of metal monohydrides including loss of H·,[35] reductive elimination of HCl,[36] loss of other ligands,[37] and isomerization.[37] Three possible photochemical reactions could be envisaged for **1** leading to (a) H loss, (b) ring slip and ligand gain, and (c) hydrogen migration and ligand gain:

$$ReCp_2H \rightarrow ReCp_2 + H \quad (12a)$$

$$ReCp_2H \xrightarrow{L} ReCp(H)L(\eta^3\text{-}C_5H_5) \quad (12b)$$

$$ReCp_2H \xrightarrow{L} ReCp(L)(\eta\text{-}C_5H_6) \quad (12c)$$

The matrix experiments on **1** prove that the first two pathways occur but not the third.

The first pathway is accessible only in CO and N_2 matrices; apparently, the reverse reaction prevents its observation in Ar matrices. In CO the released hydrogen atoms are trapped by the matrix, but N_2 does not provide any trapping action. The lack of **4** in Ar matrices suggests that the H atom is expelled with little excess energy. The production of **4** by prior coordination of CO/N_2 followed by reductive elimination of HCO/HN_2 is implausible and incompatible with results obtained from mixed Ar/CO matrices. We encountered surprising difficulty in proving that hydrogen loss is isotopically selective when using $ReCp_2D$ and $Re(\eta\text{-}C_5D_5)_2H$. The sources of these problems seem to lie (i) in the photosensitivity of HCO, which may lead to exchange reactions, and (ii) in the IR absorptions of DCO, which are broader and less intense than those of HCO. The photodissociation of HCO is reduced but probably not eliminated by filtering out visible radiation with $CoSO_4/NiSO_4$.[38] It should be noted that the published spectrum of DCO obtained by photolysis of DI in solid CO also shows intense peaks due to HCO.[25b]

We have observed the second pathway, ring slip and ligand gain, with both N_2 and CO as the entering ligand. Experiments in reactive matrices involving ligand gain do not necessarily distinguish whether the reactions occur in two steps or one, so this part of the mechanism remains undetermined. Such $(\eta^5\text{-}C_5H_5)$ to $(\eta^3\text{-}C_5H_5)$ decoordination has been observed previously both in solution[30] and in matrices.[39] Unfortunately, the evidence for ring slip depends on the assumption that the rhenium maintains an 18-e configuration. The reversibility of the addition of CO to **1** is demonstrated both by the increased yield of **5** in dilute CO/Ar matrices and by the observation of **5** (=**11**) as an intermediate prior to formation of **1** on photolysis of **3**.

The third pathway, hydrogen migration and ligand gain, does not appear to be a primary reaction of **1**. However, its occurrence in CO matrices as a secondary step is shown by the formation of **3** in low yields. In CO-saturated solutions **3** is indeed the first observed product of photolysis of **1**. More details of this step are derived from the photochemical reactions of **3** discussed below.

Photochemical Pathways from 2 in Matrices. As expected from the solution photochemistry of **2**[12-15] and from the matrix photochemistry of $MnCp(CO)_3$ and related compounds,[17] the photolysis of **2** in inert matrices leads to reversible formation of the coordinatively unsaturated intermediate $ReCp(CO)_2$ (**7**). In dinitrogen matrices it is replaced by the well-established dinitrogen complex, **8**.[13]

Photochemical Pathways from 3 in Matrices. The photochemical reactions of most substituted metal carbonyls in inert matrices fall into two simple classes: CO loss[17,40-43] and loss of other ligands.[41-43] One of the reactions observed on photolysis of **3** was reversible loss of the η^2-cyclopentadiene ligand to form **7** (=**9**). This reaction may be compared to loss of ethene from $WCp_2(C_2H_4)$[1] or the partial decoordination of butadiene in $Fe(\eta\text{-}C_4H_6)(CO)_3$.[43] As expected, **7** was replaced in reactive CO or N_2 matrices by **2** and **8**, respectively. To our surprise, there was no evidence for CO loss as a competing pathway (cf. ref 41-43) and only slow exchange with **3** in ^{13}CO matrices; instead we found evidence for hydrogen migration to the metal to form **10**, which we assume to have a $(\eta^1\text{-}C_5H_5)$ ring in order to satisfy the 18-e rule. Only after formation of **10** did CO loss occur, so forming first **5** (=**11**) and then **1**.

The hydrogen migration in the reactions of **3** and **1** is thus shown to be

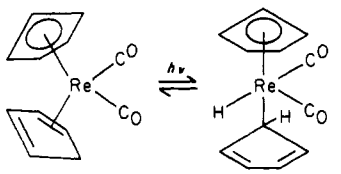

3 10

Other authors who have examined ring ⇌ metal hydrogen and alkyl migrations have often considered that they may proceed via 16-e intermediates (Scheme II), but such an intermediate has been observed only in the fourth example of Scheme II. However, in the alkyl transfer[9] of $MoCp_2(Et)Cl$, a single-step reaction seems more plausible. In our case we have observed $ReCp(CO)_2$, which would be the 16-e intermediate if the reaction proceeded by loss of C_5H_6 to form **7**, followed by oxidative addition of C_5H_6 to form **10**. The question of the intermediacy of **7** can be resolved by examining whether **10** grows after **7**. The growth curve of **7** and **10** (Figure 4) peak almost simultaneously during photolysis of **3** whereas **11** is clearly formed in a subsequent secondary reaction. However, longer wavelength photolysis does convert a small percentage of **7** into **10**. We conclude that the conversion of **3** into **10** occurs mainly by a direct hydrogen transfer in a single step but that a minor pathway exists through the intermediacy of **7**. (A single-step reaction is taken to include very rapid reactions via undetected intermediates.) Thus, the two alternative primary photochemical reactions of **3** are hydrogen migration and cyclopentadiene loss.

Mechanism of the Photochemical Reactions of 1 and 3 in Solution. The conversion of **1** into **3** by irradiation at room temperature in CO-saturated solutions demonstrates (a) the photosensitivity of **1** in solution and (b) a close relation to the reactions of **1** in matrices. Whereas the major CO addition product in solution is **3**, this is a minor product in matrices and the reaction barely proceeds beyond the monocarbonyl **5**. Since we have established that **1** reacts both thermally and

(34) Geoffroy, G. L. *Prog. Inorg. Chem.* **1980**, *27*, 123. Green, M. A.; Huffman, J. C.; Caulton, K. G. *J. Am. Chem. Soc.* **1981**, *103*, 695.
(35) Sweany, R. L. *Inorg. Chem.* **1980**, *19*, 3512; **1982**, *21*, 753. Church, S. P.; Poliakoff, M.; Timney, J. A.; Turner, J. J. *J. Am. Chem. Soc.* **1981**, *103*, 7515. Hoffman, N. W.; Brown, T. L. *Inorg. Chem.* **1978**, *17*, 613.
(36) Geoffroy, G. L.; Gray, H. B.; Hammond, G. S. *J. Am. Chem. Soc.* **1975**, *97*, 3933.
(37) Geoffroy, G. L.; Bradley, M. G. *Inorg. Chem.* **1977**, *16*, 744.
(38) Jacox, M. E. *J. Mol. Spectrosc.* **1973**, *47*, 1418.
(39) Crichton, O.; Rest, A. J.; Taylor, D. J. *J. Chem. Soc., Dalton Trans.* **1980**, 167. Fettes, D. J.; Narayanaswamy, R.; Rest, A. J. *J. Chem. Soc., Dalton Trans.* **1981**, 2311.
(40) Poliakoff, M. *Inorg. Chem.* **1976**, *15*, 2022. McHugh, T. M.; Rest, A. J. *J. Chem. Soc., Dalton Trans.* **1980**, 2323.
(41) Boxhoorn, G.; Stufkens, D. J.; Oskam, A. *J. Chem. Soc., Dalton Trans.* **1980**, 1328. Balk, R. W.; Boxhoorn, G.; Snoeck, T. L.; Schoemaker, G. C.; Stufkens, D. J.; Oskam, A. *J. Chem. Soc., Dalton Trans.* **1981**, 1524.
(42) McHugh, T. M.; Rest, A. J.; Sodeau, J. R. *J. Chem. Soc., Dalton Trans.* **1979**, 184.
(43) Ellerhorst, G.; Gerhartz, W.; Grevels, F.-W. *Inorg. Chem.* **1980**, *19*, 67.

Scheme II

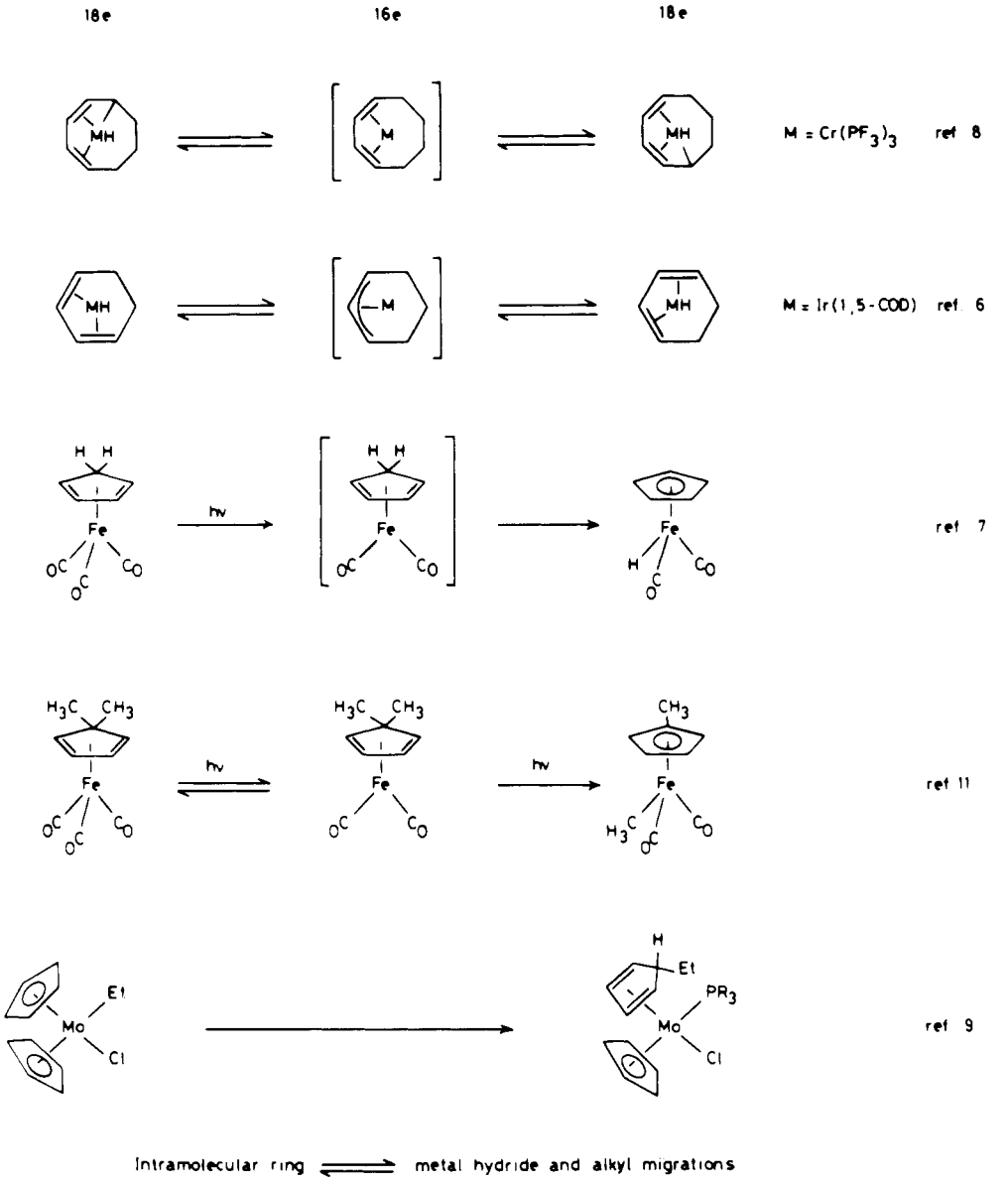

photochemically with CO in solution to form **3**, it is reasonable to postulate that this reaction follows the same route as the photochemical conversion of **3** into **1** in matrices. In that case the steps are (i, ii) double CO addition with concomitant ring decoordination (**1** → **5** → **10**; see Scheme I) and (iii) hydrogen migration to form **3** in the final step. The double CO addition is similar to the double phosphine addition to $ReCp(NO)(CO)CH_3$ to form $Re(\eta^1\text{-}C_5H_5)(NO)(CO)(CH_3)(PMe_3)_2$,[44] but Casey and Jones do not observe subsequent alkyl migration.

In the secondary stage of the solution photochemical reaction of **1** with CO, **3** is converted into **2**. This reaction is identical with that observed on photolysis of **3** in CO matrices and indicates that cyclopentadiene loss is an important reaction in both media. The results in inert matrices support a dissociative two-step pathway for this reaction.

Electronic Structure of Rhenocene (4). Like $MoCp_2$ and WCp_2,[1] monomeric rhenocene (**4**) had not been observed prior to these matrix experiments. The similarity of the IR spectra of $ReCp_2$ and $Re(\eta\text{-}C_5D_5)_2$ to the spectra of WCp_2, $FeCp_2$, and their deuterated analogues[1,27] points to a parallel sandwich structure for **4**[47] (see table of ref 18). Further support comes from the highly resolved absorption and emission spectra.[1,28] However, these spectra do not distinguish between the two possible low-spin d^5 ground states: $^2E_{2g}$ and $^2A_{1g}$. The $^2E_{2g}$ state is adopted by $FeCp_2^+$ and $Mn(\eta\text{-}C_5Me_5)_2$, while 17-e bis(arene) metal complexes adopt the $^2A_{1g}$ state.[45,46] A $^2E_{2g}$ state would be split into $\zeta = {}^5/_2$ and $\zeta = {}^3/_2$ substates by spin–orbit coupling,[45] and a vibronic transition at $(2\zeta + \nu)$, as observed for WCp_2,[1] would be anticipated. The absence of such a band in the 3000–5000-cm^{-1} region is suggestive of a $^2A_{1g}$ ground state, but confirmation must await an ESR spectrum.

The intense visible absorption band of $ReCp_2$ must be assigned to a charge-transfer transition. The low energy of this band is consistent with a ligand-to-metal transition,[48] with transfer of charge into the vacancy in the a_1 or e_2 orbital. (The first LMCT bands of $FeCp_2$ and $FeCp_2^+$ appear at 38 170 and 15 800 cm^{-1}, respectively; those of $Fe(MeCp)_2$ and Mn-

(44) Casey, C. P.; Jones, W. D. *J. Am. Chem. Soc.* **1980**, *102*, 6154.

(45) Warren, K. D. *Struct. Bonding (Berlin)* **1976**, *27*, 45 and references therein.

(46) Green, J. C. *Struct. Bonding (Berlin)* **1981**, *43*, 37 and references therein.

(47) A detailed comparison of the vibrational frequencies of $ReCp_2$ and other metallocenes will be published elsewhere.

(48) An estimate of the extinction coefficient of the similar UV band of WCp_2 yielded a value of $\epsilon \sim 2000$ dm^3 mol^{-1} cm^{-1}.

$(MeCp)_2$ appear at 41 250 and 24 390 cm^{-1}, respectively.[29,49] Both $^2A_1$ and $^2E_2$ ground states lead to allowed transitions.[45]) The most probable vibrational mode for the progression of such an allowed transition is the a_{1g} symmetric Cp-Re-Cp stretching mode, ν'_4.

On irradiation into this absorption, a laser-excited fluorescence (LEF) spectrum is obtained, which allows us to identify the (0, 0) transition and ν''_4. This appears to be the first observation of a LEF spectrum of a metallocene, although emission from ferrocene has been detected previously.[28] The most remarkable feature of the LEF spectra is the occurrence of bands between 20 140 and 20 370 cm^{-1}, which are to short wavelength of the first absorption maximum and must therefore be assigned to $1' \rightarrow 0''$ transitions. Their presence and the absence of higher frequency bands implies that $v' > 2$ to $v' = 1$ relaxation is much faster than the fluorescence lifetime, τ_f, but that relaxation from $v' = 1$ to $v' = 0$ occurs on a time scale comparable to that of τ_f. Since vibrational relaxation of polyatomic molecules is usually rapid, this observation suggests that τ_f may be in the picosecond-nanosecond range. It follows from this assignment that the intense bands between 19 500-20 040 cm^{-1} are the $0' \rightarrow 1''$ and $0' \rightarrow 0''$ transitions. The $0' \rightarrow 0''$ transitions of the three progressions are then 20 026 (C), 19 919 (D), and 19 860 cm^{-1} (E), compared with a value of 20 080 cm^{-1} for the first absorption band. The small discrepancies are probably associated with the site selectivity of the laser and the variations in phonon coupling. The three progressions may represent three different matrix sites. The presence of the zero phonon lines in the LEF spectrum with 465.8-nm excitation gives a value of 330 ± 2 cm^{-1} for the $\nu'_4 = 1$ to $\nu'_4 = 0$ separation, compared with a value of 332 ± 5 cm^{-1} derived from the first two members of the absorption progressions. Using the average value for the $0' \rightarrow 0''$ and $0' \rightarrow 1''$ transitions from all three emission progressions, we obtain a value of $\nu''_4 = 327$ cm^{-1}, indicating a minimal change from ν'_4.

The information about ν_4 allows some conclusions concerning the other skeletal modes of $ReCp_2$. Surprisingly, $\nu_4(a_{1g})$ exceeds both antisymmetric modes (ν_{11} and ν_{21}) observed in the IR spectrum. In order to avoid an excessive interaction force constant,[50] it is most reasonable to assign the low-frequency IR spectrum as $\nu_{11}(a_{2u}) = 316$ cm^{-1} and $\nu_{21}(e_{1u}) = 289$ cm^{-1}. Comparisons with IR spectra of other metallocenes in matrices will be made elsewhere.[23]

Conclusions

The matrix studies on **1** demonstrate that this metal hydride exhibits a remarkable photochemistry with two competing pathways, hydrogen loss and ring slip with ligand gain. The first reaction leads to the new metallocene **4**, which shows structured visible-absorption and laser-excited emission spectra. The second leads in solid CO to a monocarbonyl that is the first intermediate en route to **3**. Photolysis of **2** leads to coordinatively unsaturated **7**, which may then be identified as one of the products of **3**. Competing with reversible cyclopentadiene loss to form **7**, the complex **3** undergoes one-step oxidative hydrogen transfer to **10** before losing CO in two steps to return to **1**. The monocarbonyl intermediate **5** is identical with the CO-gain product of **1**. Solution reactions of **1** lead to **3** with both photochemical and thermal activation, suggesting that **5** and **10** are also intermediates in solution. As in the matrix, photochemical loss of cyclopentadiene from **3** in CO-saturated solution leads to **2** via a dissociative mechanism. In future studies we will attempt to exploit the synthetic potential of the solution photochemistry of **1** and search for further solution intermediates.

Acknowledgment. We are grateful to Drs. A. J. Downs and M. L. H. Green for many discussions and for the use of apparatus. We thank the SERC for support and for a studentship (P.G.).

Registry No. **1**, 1271-32-5; **2**, 12079-73-1; **3**, 79471-01-5; **4**, 56261-86-0; **5**, 56261-86-0; **6**, 85283-44-9; **7**, 85283-45-0; **8**, 36543-62-1; **10**, 85283-46-1.

Supplementary Material Available: Table I, showing IR frequencies of the precursors **1**, **2**, **3**, and cyclopentadiene (2 pages). Ordering information is given on any current masthead page.

(49) Gordon, K. R.; Warren, K. D. *Inorg. Chem.* **1978**, *17*, 987.

(50) This argument assumes a linear triatomic model for $ReCp_2$ (cf. ref 27).

Notes

Contribution from the Department of Chemistry, University of Houston, Central Campus, Houston, Texas 77004, and University of California, Los Alamos National Laboratory, Los Alamos, New Mexico 87545

Synthesis and Studies of Poly(aminoborane), $(H_2NBH_2)_x$

Richard Komm,[1] R. A. Geanangel,*[1] and Rai Liepins*[2]

Received October 11, 1982

Even though a substance believed to be polymeric H_2NBH_2 was first reported over 40 years ago[3] and more information on its preparation and properties appeared over the following two decades,[4-7] a detailed characterization was lacking until Shore and co-workers demonstrated that two distinct types of materials exhibit the composition BNH_4.[8,9] Crystalline $(H_2NBH_2)_n$ (n = 2-5) cycloborazane molecules are formed in the reaction of $NaNH_2$ with $BH_2(NH_3)_2^+BH_4^-$ in liquid NH_3[8] while the reaction of $LiNH_2$ with B_2H_6 in $(C_2H_5)_2O$ affords nonunique amorphous materials[7,9] apparently containing 3-5 NH_2BH_2 units solvated in an undetermined manner. A direct synthesis of $(H_2NBH_2)_3$ from borazine was reported by Dahl and Schaeffer.[10]

Another reported preparation of poly(aminoborane) involved subjecting borazine vapor to a radio-frequency discharge, forming monomeric H_2NBH_2 (among numerous other prod-

(1) University of Houston.
(2) Los Alamos National Laboratory.
(3) Schlesinger, H. I.; Ritter, D. M.; Burg, A. B. *J. Am. Chem. Soc.* **1938**, *60*, 2297.
(4) Wiberg, E.; Hertwig, K.; Bolz, A. *Z. Anorg. Allg. Chem.* **1948**, *256*, 177.
(5) Wiberg, E.; Boltz, A.; Buchheit, P. *Z. Anorg. Allg. Chem.* **1948**, *256*, 285.
(6) Schaeffer, G. W.; Basile, L. J. *J. Am. Chem. Soc.* **1955**, *77*, 331.
(7) Schaeffer, G. W.; Adams, M. D.; Koenig, F. J. *J. Am. Chem. Soc.* **1956**, *78*, 725.
(8) Böddeker, K. W.; Shore, S. G.; Bunting, R. K. *J. Am. Chem. Soc.* **1966**, *88*, 4396.
(9) Denton, D. L.; Johnson II, H. D.; Hickam, C. W., Jr.; Bunting, R. K.; Shore, S. G. *J. Inorg. Nucl. Chem.* **1975**, *37*, 1037.
(10) Dahl, G. H.; Schaeffer, R. *J. Am. Chem. Soc.* **1961**, *83*, 3032.

0020-1669/83/1322-1684$01.50/0